Hindawi
International Journal of Polymer Science
Volume 2021, Article ID 1907914, 9 pages
https://doi.org/10.1155/2021/1907914

Research Article

Application of Fish Collagen-Nanochitosan-Henna Extract Composites for the Control of Skin Pathogens and Accelerating Wound Healing

Ahmed A. Tayel,[1] **Reem A. Ghanem**,[1] **Mohammed S. Al-Saggaf**,[2] **Dalia Elebeedy**,[3] **and Ahmed I. Abd El Maksoud**[4]

[1]*Faculty of Aquatic and Fisheries Sciences, Kafrelsheikh University, Egypt*
[2]*College of Science and Humanitarian Studies, Shaqra University, Quwaiiyah 11971, Saudi Arabia*
[3]*College of Biotechnology, Misr University for Science and Technology (MUST), 6th of October City, Egypt*
[4]*Genetic Engineering and Biotechnology Research Institute, University of Sadat City, Egypt*

Correspondence should be addressed to Ahmed A. Tayel; tayel_ahmad@yahoo.com

Received 22 April 2021; Revised 3 June 2021; Accepted 15 June 2021; Published 30 June 2021

Academic Editor: Marta Fern ndez Garc a

Skin is the largest protective organ that could be recurrently wounded and attacked by microorganisms. The wounded skin safeguarding and supporting were intended through natural derivatives. Fish collagen (Cg) type I, extracted from sea bream (*Spondyliosoma cantharus*), chitosan nanoparticles (NCht) from shrimp shells, and henna (*Lawsonia inermis* L.) leaves extract (He) were produced and physiochemically characterized. The antimicrobial potentialities of these compounds and their composites were assessed toward skin pathogens (*Candida albicans* and *Staphylococcus aureus*) using various assaying methods and microimaging techniques. The infrared and electrophoretic analysis of Cg validated its characteristics, and the IR-spectroscopic analysis of the compounds/composites indicated their physiochemical attributes and interrelations. The produced NCht particles had a diameter range of 64.6-308.8 nm, 104 nm mean diameter, and +31.3 mV zeta potentiality. Both NCht, He, and NCht/He composite exhibited significant antimicrobial potentiality toward skin pathogens; NCht/He was the strongest with inhibitory concentrations of 20.0 and 22.5 μg/mL and inhibition zones of 25.7 and 26.8 mm against *S. aureus* and *C. albicans*, respectively. The electron micrographs verified the synergistic microbicidal action of NCht/He, as they led to severe microbial lysis and deformations. The skin wounds' treatment with NCht/He/Cg composite promoted the fastest and complete healing of wounded rats' skin during 8 days of local treatment, with the absence of inflammation and infection signs; treated with NCht/He/Cg composite, the wound area vastly reduced from 63.6 mm^2 to 15.9 and 9.1 mm^2 after 2 and 4 days, respectively. The natural NCht/He/Cg composites are recommended as topical applications for optimum skin disinfection and regeneration.

1. Introduction

Skin is the outmost and largest organ, which covers all the body; the skin's utmost role is the protection of muscles, bones, ligaments, and interior organs from external threats, including biological, physical, chemical, and mechanical agents [1]. However, wounds, illnesses, burns, or surgical incisions can dangerously affect the structure/functions performed by the skin; the main threat challenge for wounded skin caregivers is the microbial infections and inflammation emergence in injured tissues [2].

Although numerous medications were introduced for remediate and regenerate wounded skin, the accustomed antibiotic prophylaxis and anti-inflammatory drugs were not sufficient to overcome wound contamination and inflammation with skin's bioburden microorganisms [3].

Collagen (Cg) constitutes the foremost structural fraction of skins' extracellular matrix and the utmost researched biopolymer for tissue regeneration/engineering applications [4]. The Cg-based dressings were effectually employed for accelerating skins' wound healing (WH), which are attributable to the swelling capacity, high biocompatibility,

biodegradability, facile adherence, and powerful protection of wounds' bed [5].

From ~27 identified Cg types (classified with function, distribution, size, and composition amino acids), type I Cg is the principal for human skin care and industrial/cosmetic applications; it designates 2 alpha "α1 and α2" and 1 beta "β" peptide chain, with elevated tensile stiffness and stability [6]. The traditional Cg sources, e.g., porcine and bovine Cgs, have currently many problematic concerns for applications in biomedical and cosmetic disciplines, such as religious issues and diseases' transmission risks. Thus, fish Cg introduced splendid alternatives for applications in biomedicine, tissue engineering, skin care, and regeneration, with higher biocompatibility to human and minimum disease transmission risk [7–9].

The biopolymers are greatly valuable with paramount importance for applications in environmental, pharmaceutical, biomedical, and many other health promotion disciplines [10]. Due to their biocompatible, biodegradable, ecofriendly, and bioactive properties, biopolymers and their blends (e.g., chitosan, natural gums, alginate, carrageenan, fucoidan, mucilages, pectin, and cellulose) were applied, either individually or after structural modifications, in drug delivery and bioactive molecules carrying to treat various superficial and internal human disorders [10–14].

From the astonishing bioactive natural biopolymers is chitosan (Cht), which is derived from chitin N-deacetylation, they both constitute the principal supporting components in crustaceans shells, most insects, and fungi cell walls [10, 15]. The Cht is confirmed to possess superior bioactivities, e.g., antimicrobial action, antioxidant, WH acceleration, tissue engineering, biochelation, biosorption, anti-inflammatory, anticancer, and drug-carrying capabilities [15–20]. The Cht was introduced as an effectual base for applications in skin care/regeneration, wound dressing, and tissue engineering [19, 21]; the Cht main advantages depend on its combined unique characteristics such as biocompatibility, biodegradability, nontoxicity, and high adsorption capacity. The bioactivities of Cht are much augmented by its transforming into nanoforms, which provides it with greater reacted surfaces and charges to become more effective for WH, microbial inhibition, drug-carrying capabilities, and radical scavenging [22–26].

Henna "*Lawsonia inermis* Linn" is amongst the most cosmetically important dyes providing plants cultivated worldwide; henna leaves powder/extract were historically applied for decorating skin, fingernails, hair, leathers, and textiles [27, 28]. As henna contains treasures of bioactive constituents (e.g., lawsone, naphthoquinone, coumarins, phenolics, flavonoids, alkaloids, tannins, quinones, terpenoids, and xanthones), these plant derivatives were experimented in numerous medicinal, pharmaceutical, and biomedical applications (including their hypoglycemic, immune stimulant, analgesic, hepatoprotective, anticancer, anti-inflammatory, antimicrobial, antidermatophytic, antiparasitic, antisickling, antitrypanosomal, antioxidant, allelopathic, and wound healing activities) [29–32]. The WH activity and reducing inflammation and infections of wounded skins were reported from henna extracts (He) [30, 33–35]. The fabrications of wound dressing/WH accelerator formulations based on biopolymers/nanopolymers and plants' extracts were suggested as effectual treatments for healing injured tissues and prevent their inflammation/infections, either individually or in composited forms [3, 23, 36–38].

Accordingly, the aims/objectives of the research are the extraction of Cg from sea bream fish, Cht nanoparticles (NCht), and henna extract (He) and the assessment of produced agents and their conjugated composites as antimicrobial (against skin pathogens) and WH accelerators in wounded rats.

2. Materials and Methods

2.1. Chemicals and Reagents. The entire chemicals/reagents used in experiments were attained from certified companies and were analytical grades. The sodium hydroxide (NaOH), hydrochloric acid (HCl, 37%), acetic acid (CH_3COOH), sodium chloride (NaCl), sodium-tripolyphosphate (TPP), ethanol (C_2H_5OH) ketamine ($C_{13}H_{16}ClNO$), vancomycin, and nystatin were gotten from Sigma-Aldrich Co. (St. Louis, MO, USA), whereas the microbiological media, YM "yeast-malt extract agar/broth," and TS "trypticase soy agar/broth" were gotten from Difco Laboratories (Detroit, MI, USA).

2.2. Fish Collagen (Cg) Extraction and Characterization. By-products of sea bream (*Spondyliosoma cantharus*) filleting, e.g., fish skins, were obtained from "Kafrelsheikh University Fish Processing Research Plant"; collected samples were retained at -20°C until thawing and subjecting to extraction. The extraction process depended on illustrated protocol [39], with minor adjustments. The entire steps were executed at temperature of ≤4°C using DW "double-distilled water" to dissolve and wash. In brief, cut skin into ~2 cm^2 parts was extensively washed; then, skin's noncollagenous proteins were deproteinized via immersion in 20 folds (w/v) of 0.1 N NaOH, stirring for 18 h, and rewashing. Cg was extracted in 25 folds from 0.5 M acetic acid for 48 h, followed by filtration and precipitation with 1.0 M NaCl treatment. Precipitated acid soluble Cg was harvested by centrifugation for 45 m at 18.500 × g, lyophilization of harvested pellets then dialysis against acetic acid (0.1 M) and DW. The Cg characterization involved SDS-PAGE "SDS-polyacrylamide gel electrophoresis" for appraising structural peptide molecular weight (MW) and FTIR spectroscopic analysis "Fourier transforms infrared-JASCO spectrometer 4100, Tokyo, Japan" for detecting biochemical structural bonds of the compound [40].

2.3. Shrimp Shell Nanochitosan Preparation. Cts was extracted from shrimp (*Penaeus monodon*) waste exoskeletons, obtained from the "Aquaculture Research Farm, Kafrelsheikh University, Egypt", as demonstrated [41]. Briefly, shrimp flesh was detached; then, exoskeletons (shells) were washed repeatedly with DW and dried, at 50 ± 2°C for 22 h, and mechanically pulverized. The Cht extraction involved the following: (1) deproteinization: in 25 folds (w/v) from 0.1 M NaOH at 70 ± 2°C for 125 min then recurrent DW washing; (2) demineralization: treatment of deproteinized

materials with 25 folds (w/v) from 0.2 M HCl for 22 h to have chitin after recurrent DW washing and drying; (3) deacetylation: via chitin treatment with 30 folds (w/v) from 62% NaOH solution for 90 min at 118°C. After cooling, alkali drainage, and Cht extensive DW washing, Cht was dried 50 ± 2°C for 18 h then analyzed. The Cht was analyzed with FTIR, and its deacetylation degree (DD) was estimated from the IR spectrum [42], whereas the Cht molecular weight (MW) was assessed using HPLC "high-performance liquid chromatography, Agilent-LC 1100, CA" [43].

The Cht nanoparticle (NCht) preparation was conducted using TPP, as illustrated [44]. Cht solution (2.5 mg/mL) dissolved in 1.0% (v/v) aqueous CH_3COOH solution was made, with adjusted pH to 5.5. TPP solution (1.25 mg/mL) in DW was freshly prepared, and equal volume was dropped slowly (~300 μL/min) into Cht solution, while subjected to vigorous stirring without heating. Stirring was continued for extra 90 min after finishing TPP dropping; then, the mixture was sonicated, frozen, and lyophilized.

2.4. Extraction of Henna Leaves. Fresh identified henna leaves (*Lawsonia inermis* L.) were attained from ARC "Agricultural Research Center, Giza, Egypt", cleansed, hot air-dried (45 ± 2°C), and mechanically powdered. Henna powder (~100 g) was soaked in 65% C_2H_5OH (ethanol, 1200 mL) and frequently agitated for 56 h, without heating. Plant residues were excluded by filtration through Whatman No. 1 paper, and the extraction filtrates were flash evaporated "Büchi, Flavil, Switzerland" at 44°C until dryness. The resulted He was redissolved via agitation for 24 h in DW to have 10% concentration.

2.5. Test Organisms. Skin microbial pathogens "*Candida albicans* (ATCC-10231) and *Staphylococcus aureus* (ATCC-25923)" were employed to judge the products' antimicrobial activity. The microbial cultures were propagated and challenged aerobically at 37°C using YM for *C. albicans* and TS for *S. aureus*.

2.6. Antimicrobial Assays. The appearance of IZ "growth inhibition zones" was considered as an indicator for antimicrobial activity from NCht, He, and their composites using disc-diffusion assay [45]. Diluted solutions of produced agents (NCht, He, and NCht/He composite) were impregnated onto sterile discs (0.6 cm diameter), which were positioned onto the surfaces of inoculated agar plates with microbial cultures and incubated for 18-24 h. Plates (triplicated) were incubated at 37°C, and the IZ diameters' means were considered.

The MIC "minimal inhibitory concentration" measurement from each agent/composite toward skin pathogens was performed as indicated by Tayel et al. [16], through a microdilution method and 10-100 μg/mL concentration range of screened agents (NCht, He, and NCht/He composite) in microbial liquid media. The customary antibiotics (nystatin and vancomycin) were employed as positive controls for comparison.

2.7. Wound Healing (WH) Potentiality of Composited Materials. Young Wistar healthy rats (average weight between 142 and 166 g) were individually housed under maintained conditions "25 ± 2°C; 12 h of light-dark cycle; 65 ± 3% relative humidity" in polyethylene clean cages. Animal handling and practical experiments were implemented following the guidelines of the "Kafrelsheikh University Ethical Committee for the care and use of laboratory animals" with the aid of two veterinarian technicians. The experiment period lasted for 14 days, with rats feeding on a customary pellet diet and free water access. After anesthesia induction via ketamine intramuscular injection (100 mg/kg body weight), wounds with semicircular areas of ~60 mm^2 were made on shaved rats' thoracic area. From the wounding day (day 0), the experimented composites (containing 1.0% NCht + 1.0% He (T1 group) and 1.0% NCht + 1.0%He + 1.0% Cg (T2 group), dissolved in DW) were topically smeared every 12 h until complete epithelization. Wounds were digitally photographed daily; the reductions and manifestation of wounded areas were appraised from the captured photographs.

2.8. Statistical Analysis. The means ± SD "standard deviations" from triplicated experimentations were computed (Microsoft Office-Excel sheets 2013), and the significance analysis between results was executed electronically (MedCalc statistical software (V. 15.2), Belgium) at ≥95% CI.

3. Result and Discussion

3.1. Fish Cg Characterization. Fish Cg was effectually produced from sea bream shin, with 32.4% dry weight yield; this yield is in the average range of Cg extracted from other fish wastes, using acid solubilizing technique [39, 46]. The structural attributes of produced Cg, including its FTIR spectrum and SDS-PAGE pattern, are illustrated in Figure 1. As appointed in Figure 1-(1), the main characteristic bands for Cg were observed, especially the corresponding band to amide A, amide B, and amides I, II, and III, at 3331, 2922, 1658, 1593, and 1239 cm^{-1}, respectively. The detected bands and their wavenumbers are closely related to formerly reported representative bands for fish Cg, in close spectral wavenumbers to current findings [46–48].

The characterization of Cg by SDS-PAGE (Figures 1–2) exemplified that extracted Cg type had harmonized polypeptide chains, containing two α chains (α1and α2); the α1 band had a higher density than α2 band, with respective MWs of ~111.2 and 122.7 kDa, respectively. The β chain also appeared in the Cg pattern. These characteristic polypeptide chains indicate that produced Cg belonged to type I [6, 36, 49].

3.2. NCht Characterization. The extracted Cht powder from *P. monodon* shells had a creamy color, a MW (molecular weight) of 162.3 kDa, and a 91.2% DD. The DD (higher than70%) and the estimated MW of shrimp Cht verified the chitin transformation to Cht with ~low MW [15]. The synthesis of NCht from shrimp Cht was achieved, and the characterization of produced polymer nanoparticles revealed that the Ps ranges from 64.6 nm to 308.8 nm with mean Ps diameter of 104.3 nm.

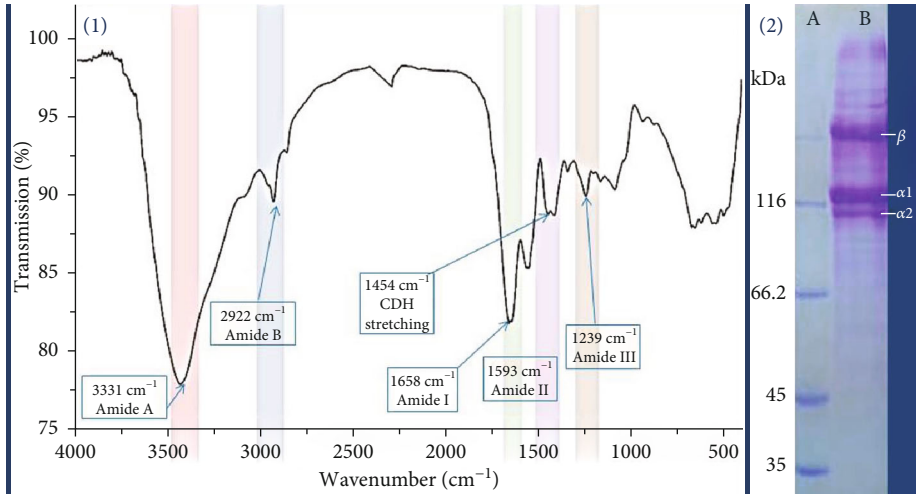

Figure 1: FTIR spectrum (1) and SDS-PAGE electrophoresis pattern (2) of fish collagen produced from *Spondyliosoma cantharus*.

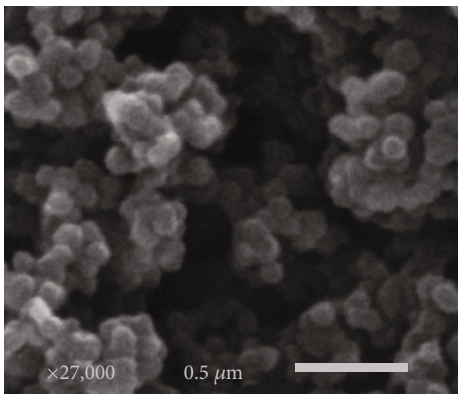

Figure 2: SEM micrograph of synthesized chitosan nanoparticles.

The NCht particles were positively charged (zeta potential of +31.3 mV) and had homogenous, well dispersion, and spherical contours, as evidenced by their SEM imaging (Figure 2).

3.3. FTIR Analysis. The FTIR spectral assessment for NCht and He and the composites of NCht/He and NCht/He/Cg are presented (Figure 3). The NCht spectrum had the key characteristic bands that are designated in standard Cht (Figure 3, Cht). The main NCht characteristic peaks were distinguished at 1071 cm^{-1} (C–O stretch), 1375 (bridge O stretch), 1658 and 1630 (N–H bend), 2924 (C–H stretch), and 3440 (–OH stretch) [36]. In the FTIR spectra of He (Figure 3, He), the broad and strong peak observed at 3431 cm^{-1} is attributed to vibrated stretching of –OH groups; the two peaks at 2925 and 2830 cm^{-1} were assigned to vibrated stretching of –CH_2, and the peak at 1650 cm^{-1} indicated the carboxylate anions (–COO–), whereas the weak peak appeared at 1467 cm^{-1} indicated N–H vibrated stretching in He amide [50, 51].

The interaction between NCht and He was illustrated (Figure 3, Cht/He); this involved intermolecular hydrogen bonding of the hydroxyl and carbonyl group in He with the hydroxyl and amino group of NCht, respectively. The first peak had less sharpness and stretching, with a lower frequency of 3406 cm^{-1} of (OH) groups, and the stretching band of 1650 cm^{-1} was shifted to higher wavenumber of 1629 cm^{-1} in NCht/He composite [52, 53].

After Cg addition to NCht/He composite, the He characteristic peaks were mostly overlapped with Cg. However, a novel peak was immerged at around 3697 cm^{-1}, the characteristic band for Cg amide B mostly disappeared, the band of Cg amide I also shifted to lesser wavelength whereas the amide II stretching was shifted to higher wavelength, and amide III showed more shrinking [6, 49]. These apparent alterations in composited agents' structures indicate the biochemical interactions between most of these agents, i.e., NCht, He, and Cg [38].

3.4. Antimicrobial Potentiality. Table 1 depicts the *in vitro* antimicrobial potentialities of NCht, He, and NCht/He composite against *C. albicans* and *S. aureus*. The inhibitory actions varied from examined agents; the most significantly powerful treatment was the challenge with NCht/He composite, as evidenced with its widest ZOIs and least MICs toward both skin pathogens (Table 1). The He exhibited also strong antimycotic and antibacterial potentialities, and their conjoining with NCht synergistically augmented their activity. Interestingly, no significant differences were calculated between the ZOIs from NCht/He composite and nystatin (toward *C. albicans*) and vancomycin (toward *S. aureus*), which indicates the higher potentiality of composite compared to customary standard antibiotics. The He dose-dependent antimicrobial activity was reported and attributed to its high contents from glycosides and flavonoids, which are well-recognized as potent antimicrobial compounds [38, 54, 55]. Additionally, the lawsone (as a major constituent in He) was verified to possess strong antimycotic and microbicidal actions toward numerous screened pathogens [56]; these pathogens included *S. aureus* and other Gram-positive/negative bacteria [57]. Regarding NCht, it has the main antimicrobial attributes of bulk Cht (e.g., positive charged

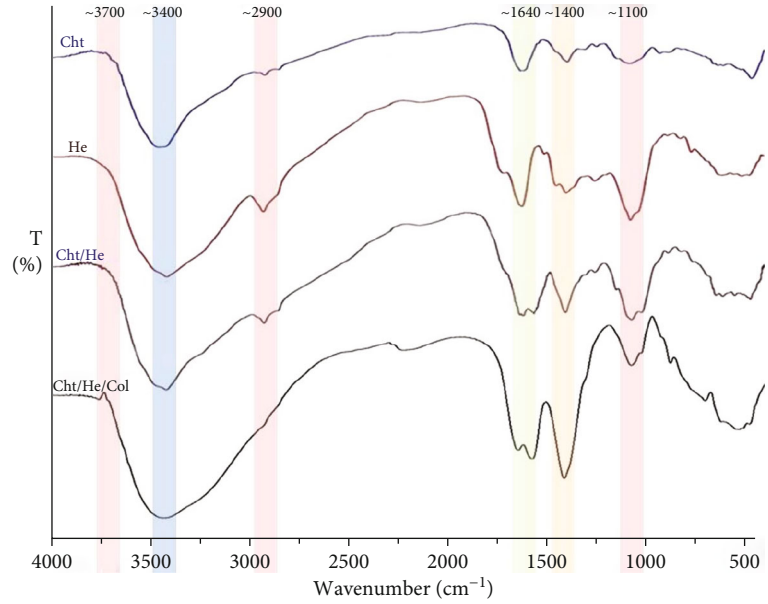

Figure 3: FTIR spectra of nanochitosan (Cht), henna extract (He), and their composites alone (Cht/He) and with collagen (Cht/He/Col).

Table 1: Antimicrobial activity of synthesized agents against shin pathogens measured as zone of inhibition (ZOI, mm)* and minimal inhibitory concentrations (MIC, μg/mL).

Agent	*Candida albicans*		*Staphylococcus aureus*	
	ZOI**	MIC	ZOI	MIC
He	23.4 ± 1.6^{a}	27.5	21.6 ± 1.4^{a}	30.0
NCht	14.6 ± 0.8^{b}	45.0	12.9 ± 0.6^{b}	47.5
NCht/He	26.8 ± 1.9^{c}	22.5	25.7 ± 1.7^{c}	20.0
Vancomycin	ND***	ND	26.8 ± 2.1^{c}	15.0
Nystatin	27.4 ± 2.3^{c}	17.5	ND	ND

*"Inhibition zones impart triplicates' diameter means ± SD, assay discs (6 mm diameter) carried 50 μg from henna extract (He), nanochitosan (NCht), their blend (NCht/He), or standard antibiotic". **"Dissimilar superscript letters within the same column indicated significant difference at $p < 0.05$.". ***ND: not detected.

particles, attachment to cells' membranes, interaction with intercellular components like DNA, and inhibition of their activities), but NCht particles have these attributes in superior manners, which make them ideal antimicrobial candidates [16, 18, 24, 25].

The bioactivities of NCht (e.g., antimicrobial, anticancer, and preservative attributes) were illustrated to be augmented via nanopolymer incorporation with additional bioactive phytocompounds [18, 26, 41, 58], which appointed the biocompatibility and synergy behavior of NCht when joining with other bioactive molecules.

3.5. Microbicidal Action. The consequences of exposure to NCht/He composite on the constructions of skin pathogens *C. albicans* and *S. aureus* after different durations are shown in Figure 4. Regarding control cells (Figure 4, C-0 and S-0), which appeared with contacted, smooth, and uniformed surfaces, the treated pathogens' cells with NCht/He composite for 5 h had obvious morphological alterations and distortions, accompanied with observable lysis signs (Figure 4, C-5 and S-5). After 10 h of exposure, the cells were mostly lysed and released their interior components, especially for *C. albicans* cells (Figure 4, C-10). The *S. aureus* cells' residues were remarkably coalesced as consequences of their membrane lysis (Figure 4, S-10). The NCht was comprehensively reported to exhibit powerful antimicrobial actions for fighting microbial pathogens; the main action resulted from NCht surface charges (positive), which enable its attachment to microbial surfaces, deform them, and interfere their permeability [24, 25, 59]. The nanosized NCht particles could also penetrate into microbial cells and interact with their functional components (e.g., polymerization enzymes, DNA, RNAs, proteins, and enzymes) to inactivate them and prohibit well-organized cell membrane synthesis [24, 60, 61]. The He contains numerous bioactive constituents that have elevated antimicrobial and cytotoxicity properties against microbial cells, e.g., 1,4-naphthoquinone analogues, lawsone, esculetin, isoplumbagin, hennadiol, laxanthone, lupeol, lacoumarin, fraxetin, betulinic acid, scopoletin, betulin, and flavone glycosides [27, 55, 56, 62]; most of these compounds have diverse microbicidal actions affected the synthesis and development of cells' vital and structural organelles.

Accordingly, the compositing of these two powerful antimicrobials (NCht and He) led to forceful synergistic action that could effectually destroy the bacterial and yeast pathogens, in a time-dependent manner. This attribute was reported for NCht when incorporating with other bioactive phyto and natural compounds [20, 24, 41, 58].

3.6. Wound Healing Acceleration. The consequences of treatment rats' wounded skin with NCht/He composite (T1) and NCht/He/Cg composite (T2) on the healing rate of wounds

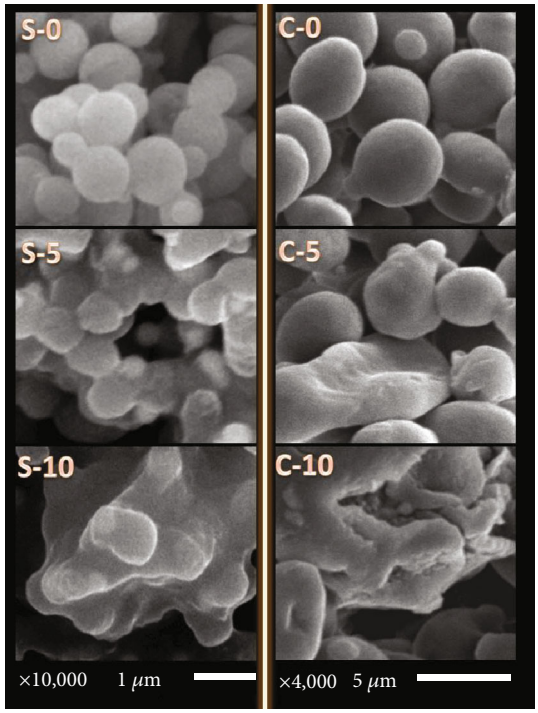

Figure 4: Consequences of exposure to nanochitosan/henna extract composite on the constructions of skin pathogens *C. albicans* (C) and *S. aureus* (S) after 0, 5, and 10 h of treatment.

throughout 8 days, compared to untreated (C) wounds, were photographically illustrated (Figure 5).

The skin wounds' treatment with NCht/He/Cg composite promoted the fastest healing of wounded rats' skin during 8 days of local treatment (Figure 5). For the untreated group (Figure 5, C), no complete healing was observed after 8 days, and the mean wound size reduced from 57.3 mm^2 to 52.8, 46.5, 38.5, and 23.4 mm^2 after 2, 4, 6, and 8 days, respectively. The healing signs appeared faster in the T1 group, treated with NCht/He composite (Figure 5, T1); the wounded parts became mostly healed after 8 days of treatment.

In the T2 group, treated with NCht/He/Cg composite, the wound area vastly reduced from 63.6 mm^2 to 15.9 and 9.1 mm^2 after 2 and 4 days, respectively. The mostly complete healing was detected after 6 days of treatment (Figure 5, T2).

The wound size reduction and their closure are principally resulting from the antimicrobial, reepithelialization, and anti-inflammatory actions of the composite components, i.e., NCht, He, and Cg [63, 64].

The usage of natural derivatives for WH, as alternatives to chemotherapy, attained great concerns to manage skin infections and promote its regeneration [65]. Chitin and Cht were supposed to enhance healing process in wounded skins; the multiple monosubunits (N-acetyl glucosamine), in these polymers' compositions, are an imperative constituent in dermal tissue and have vital necessity for repairing scar tissues [19]. The Cht surface has numerous free amine groups, which can conjoin with blood acidic groups and enhance their coagulation [22]. Cht and NCht molecules (by their high positive charge) can effectively promote cells'

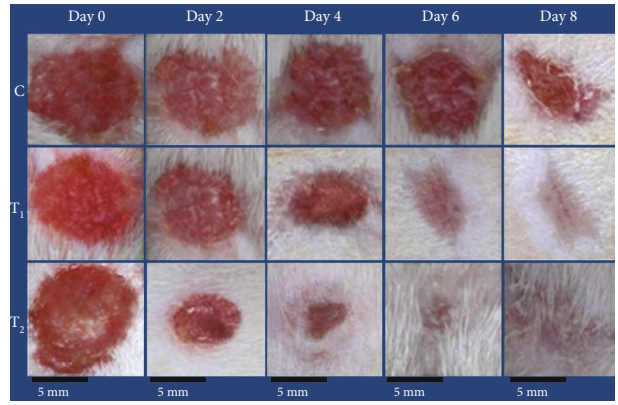

Figure 5: Consequence of rats' wounded skin treatment with nanochitosan/henna extract composite (T1) and nanochitosan/henna extract/fish collagen composite (T2) on the healing rate of wounds throughout 8 days, compared to untreated (C) wounds.

growth and assist thrombosis/blood coagulation, which greatly foster damaged tissue repairing [12, 19, 66].

The NCht potentiality was suggested for developing dressing that has high ability to remove necrotic tissues and accelerate hemostasis activity in wounded skins, which led to rapid skin regeneration and WH [23]. Polymer-based nanomaterial, e.g., NCht, was therapeutically employed for developing WH dressings or as carriers for delivering skin care biomolecules [54]; the NCht skin curative actions were attributed to its reepithelialization, anti-inflammatory, and antimicrobial properties [24, 63, 64]. The bioactivities of NCht are frequently greater than native Cht because of the increment of contacted surface area (from NPs) with microbial pathogens and injured tissues [24].

Cg is normally produced by fibroblasts; it is the key responsible for triggering cell migration and contributes to tissues' regeneration via stimulating specific cells (e.g., fibroblasts and macrophages) enhancing and accelerating WH [67].

Several studies indicated the elevated potentiality of fish Cg in healing progress and wound contraction; they confirmed Cg actions for accelerating healing development and epithelization by stimulating keratinocytes' differentiation and proliferation [48, 67–70]. The Cg was proved to augment the gene expressions of TGF (transforming growth factors), FGF (fibroblast growth factor), and VEGF (vascular endothelial growth factors), which led to stimulating cutaneous tissue healing via activating/recruiting fibroblast proliferation, angiogenesis, and deriving macrophages to generate chemotactic factors [48, 65, 70].

The incorporation or individual utilization of He had significant positive impacts in wound's contraction and epithelialization in rats. He has treasures from bioactive compounds, which could contribute to healing processes of wounded skins; the combined synergistic actions of multiple He constituents are assumed to correlate with its curative beneficial effects [35]. The He phytoconstituents include phenolic amalgams (e.g., coumarins, naphthalenes, lignans, alkylphenones, xanthones, naphthoquinones, tannins, and flavonoids), alkaloids, terpenes, and steroids [28, 29, 34].

Amongst these constituents, coumarins, tannins, alkaloids, and flavonoids are the utmost involved in the WH process. Actually, owing to their edema protective and antioxidative functions, coumarins were stated to effectually ameliorate WH [70, 71]. Additionally, the He flavonoids could augment skin WH via multiple actions, e.g., their antibacterial, astringent, cell necrosis prevention, cytokine expression modulation during inflammation, angiogenesis improvement, and prostaglandin synthesis inhibition [25, 29, 33, 70]. The He tannins' contents were also documented for contributing to WH through enhancing tissue organization and regeneration; the He tannin actions mainly depend on their astringent, antioxidant, antibacterial, anti-inflammatory, and free radical biochelation activities [28, 34, 35, 72]; these actions frequently lead to stimulate keratinocyte/fibroblast proliferation, improve WH and angiogenesis, and develop rapid crust via proteins' precipitation in damaged tissue [29, 30, 35]. The He-loaded nanopolymers, e.g., PLA and gelatin nanofibers, showed additional capabilities for controlling wound infections and WH via formation of hygienic dressings [37]. The rapid WH period, after treatment with NCht/He/Cg composite, and the absence of inflammation and infection signs in treated wounds indicated the synergistic powerful action of these agents to overcome wound infections and inflammation and promote their regeneration and epithelization.

4. Conclusion

The bioactive natural compounds, Cg, NCht, and He, were extracted from their original sources and assessed as skin protectant agents through their actions as antimicrobials and WH stimulators. The composite from NCht and He had outstanding antimicrobial potentiality against skin pathogens (*C. albicans* and *S. aureus*), whereas the Cg/NCht/He composite could effectually accelerate the WH in rats' skin, without the emergence of inflammation or infection signs, which advocate the composite topical application for optimum skin disinfection and regeneration. The study's prospects could be the examination/application of further biopolymers as carriers for WH accelerators, and investigation of their biosafety and modes of action biochemically and histologically.

Data Availability

The data used to support the findings of this study are included within the article.

Conflicts of Interest

The authors declare that they have no competing interests.

Acknowledgments

The authors are greatly thankful for the mercy help and guidance from ALLAH. The appreciation is extended for the Central Lap for Aquatic Health and Safety-Kafrelsheikh University (CLAHS), for providing the essential equipment for performing the study.

References

[1] W. C. Chua, B. K. Tan, C. L. Foo, K. C. Tan, S. J. Chong, and Y. C. Khoo, "Skin tissue engineering advances in severe burns: review and therapeutic applications," *Burns & Trauma*, vol. 4, pp. 3–17, 2016.

[2] H. D. Zomer and A. G. Trentin, "Skin wound healing in humans and mice: challenges in translational research," *Journal of Dermatological Science*, vol. 90, no. 1, pp. 3–12, 2018.

[3] E. M. Tottoli, R. Dorati, I. Genta, E. Chiesa, S. Pisani, and B. Conti, "Skin wound healing process and new emerging technologies for skin wound care and regeneration," *Pharmaceutics*, vol. 12, no. 8, p. 735, 2020.

[4] C. Dong and Y. Lv, "Application of collagen scaffold in tissue engineering: recent advances and new perspectives," *Polymers*, vol. 8, no. 2, pp. 42–62, 2016.

[5] A. Gaspar-Pintiliescu, A. M. Seciu, F. Miculescu, L. Moldovan, E. Ganea, and O. Craciunescu, "Enhanced extracellular matrix synthesis using collagen dressings loaded with Artemisia absinthium plant extract," *Journal of Bioactive and Compatible Polymers*, vol. 33, no. 5, pp. 516–528, 2018.

[6] K. Yamamoto, Y. Yoshizawa, K. Yanagiguchi, T. Ikeda, S. Yamada, and Y. Hayashi, "The characterization of fish (tilapia) collagen sponge as a biomaterial," *International Journal of Polymer Science*, vol. 2015, 5 pages, 2015.

[7] Q. Li, L. Mu, F. Zhang et al., "A novel fish collagen scaffold as dural substitute," *Materials Science & Engineering. C, Materials for Biological Applications*, vol. 80, pp. 346–351, 2017.

[8] F. Subhan, Z. Hussain, I. Tauseef, A. Shehzad, and F. A. Wahid, "A review on recent advances and applications of fish collagen," *Critical Reviews in Food Science and Nutrition*, vol. 61, no. 6, pp. 1027–1037, 2021.

[9] T. Wang, L. Yang, G. Wang et al., "Biocompatibility, hemostatic properties, and wound healing evaluation of tilapia skin collagen sponges," *Journal of Bioactive and Compatible Polymers*, vol. 36, no. 1, pp. 44–58, 2021.

[10] P. Yadav, H. Yadav, V. G. Shah, G. Shah, and G. Dhaka, "Biomedical biopolymers, their origin and evolution in biomedical sciences: a systematic review," *Journal of Clinical and Diagnostic Research*, vol. 9, no. 9, pp. ZE21–ZE25, 2015.

[11] M. Iqbal and R. A. Khera, "Nanoscale bioactive glasses and their composites with biocompatible polymers," *Chemistry International*, vol. 1, pp. 17–34, 2015.

[12] M. Abbas, T. Hussain, M. Arshad et al., "Wound healing potential of curcumin cross-linked chitosan/polyvinyl alcohol," *International Journal of Biological Macromolecules*, vol. 140, pp. 871–876, 2019.

[13] D. N. Iqbal, M. Tariq, S. M. Khan et al., "Synthesis and characterization of chitosan and guar gum based ternary blends with polyvinyl alcohol," *International Journal of Biological Macromolecules*, vol. 143, pp. 546–554, 2020.

[14] D. N. Iqbal, S. Ehtisham-ul-Haque, S. Ahmad et al., "Enhanced antibacterial activity of chitosan, guar gum and polyvinyl alcohol blend matrix loaded with amoxicillin and doxycycline hyclate drugs," *Arabian Journal of Chemistry*, vol. 14, no. 6, p. 103156, 2021.

[15] S. Kim, "Competitive biological activities of chitosan and its derivatives: antimicrobial, antioxidant, anticancer, and anti-inflammatory activities," *International Journal of Polymer Science*, vol. 2018, 13 pages, 2018.

[16] A. A. Tayel, S. Moussa, K. Opwis, D. Knittel, E. Schollmeyer, and A. Nickisch-Hartfiel, "Inhibition of microbial pathogens by fungal chitosan," *International Journal of Biological Macromolecules*, vol. 47, pp. 10–14, 2010.

[17] A. A. Tayel, M. M. Gharieb, H. R. Zaki, and N. M. Elguindy, "Bio-clarification of water from heavy metals and microbial effluence using fungal chitosan," *International Journal of Biological Macromolecules*, vol. 83, pp. 277–281, 2016.

[18] A. A. Tayel, S. H. Moussa, M. F. Salem, K. E. Mazrou, and W. F. El-Tras, "Control of citrus molds using bioactive coatings incorporated with fungal chitosan/plant extracts composite," *Journal of the Science of Food and Agriculture*, vol. 96, no. 4, pp. 1306–1312, 2016.

[19] A. Moeini, P. Pedram, P. Makvandi, M. Malinconico, and G. G. d'Ayala, "Wound healing and antimicrobial effect of active secondary metabolites in chitosan-based wound dressings: a review," *Carbohydrate Polymers*, vol. 233, p. 115839, 2020.

[20] I. O. Oladele, T. F. Omotosho, and A. A. Adediran, "Polymer-based composites: an indispensable material for present and future applications," *International Journal of Polymer Science*, vol. 2020, 12 pages, 2020.

[21] Y. Zhao, Y. Qiu, H. Wang, Y. Chen, S. Jin, and S. Chen, "Preparation of nanofibers with renewable polymers and their application in wound dressing," *International Journal of Polymer Science*, vol. 2016, 17 pages, 2016.

[22] D. Archana, J. Dutta, and P. K. Dutta, "Evaluation of chitosan nano dressing for wound healing: characterization, in vitro and in vivo studies," *International Journal of Biological Macromolecules*, vol. 57, pp. 193–203, 2013.

[23] S. S. Biranje, P. V. Madiwale, K. C. Patankar, R. Chhabra, P. Dandekar-Jain, and R. V. Adivarekar, "Hemostasis and anti-necrotic activity of wound-healing dressing containing chitosan nanoparticles," *International Journal of Biological Macromolecules*, vol. 121, pp. 936–946, 2019.

[24] N. A. Rozman, W. Y. Tong, C. R. Leong, W. N. Tan, M. A. Hasanolbasori, and S. Z. Abdullah, "Potential antimicrobial applications of chitosan nanoparticles (ChNP)," *Journal of Microbiology and Biotechnology*, vol. 29, no. 7, pp. 1009–1013, 2019.

[25] M. Chandrasekaran, K. D. Kim, and S. C. Chun, "Antibacterial activity of chitosan nanoparticles: a review," *Processes*, vol. 8, no. 9, p. 1173, 2020.

[26] M. Alghuthaymi, A. Diab, A. Elzahy, K. Mazrou, A. A. Tayel, and S. H. Moussa, "Green biosynthesized selenium nanoparticles by cinnamon extract and their antimicrobial activity and application as edible coatings with nano-chitosan," *Journal of Food Quality*, vol. 2021, Article ID 6670709, 10 pages, 2021.

[27] D. K. Singh, S. Luqman, and A. K. Mathur, "*Lawsonia inermis* L.–a commercially important primaeval dying and medicinal plant with diverse pharmacological activity: a review," *Industrial Crops and Products*, vol. 65, pp. 269–286, 2015.

[28] S. Jabeen, S. Ali, M. Nadeem et al., "Statistical modeling for the extraction of dye from natural source and industrial applications," *Polish Journal of Environmental Studies*, vol. 28, no. 4, pp. 2145–2150, 2019.

[29] K. Dhaouadi, W. Meliti, S. Dallali et al., "Commercial *Lawsonia inermis* L. dried leaves and processed powder: phytochemical composition, antioxidant, antibacterial, and allelopathic activities," *Industrial Crops and Products*, vol. 77, pp. 544–552, 2015.

[30] A. M. Salih, F. H. Kakamad, R. Q. Salih et al., "Effect of *Lawsonia inermis* (henna) on wound healing in Sprague-Dawley rats: a pilot study," *Wound Medicine*, vol. 18, pp. 41-42, 2017.

[31] A. Pasandi Pour and H. Farahbakhsh, "*Lawsonia inermis* L. leaves aqueous extract as a natural antioxidant and antibacterial product," *Natural Product Research*, vol. 34, no. 23, pp. 3399–3403, 2020.

[32] K. Kumar, N. Kumar, P. Swarnima, and A. Siddiqui, "Henna (*Lawsonia inermis*) a medicinal herb: effective in sickle cell disease," *International Journal of Indigenous Herbs and Drugs*, vol. 6, pp. 1–4, 2021.

[33] B. S. Nayak, G. Isitor, E. M. Davis, and G. K. Pillai, "The evidence based wound healing activity of *Lawsonia inermis* Linn," *Phytotherapy Research*, vol. 21, no. 9, pp. 827–831, 2007.

[34] R. B. Semwal, D. K. Semwal, S. Combrinck, C. Cartwright-Jones, and A. Viljoen, "*Lawsonia inermis* L. (Henna): ethnobotanical, phytochemical and pharmacological aspects," *Journal of Ethnopharmacology*, vol. 155, pp. 80–103, 2014.

[35] K. A. Yassine, H. Houari, B. Mokhtar, A. Karim, S. Hadjer, and B. Imane, "A topical ointment formulation containing leaves' powder of *Lawsonia inermis* accelerate excision wound healing in Wistar rats," *Veterinary World*, vol. 13, no. 7, pp. 1280–1287, 2020.

[36] A. A. Tayel, R. A. Ghanem, S. H. Moussa, M. Fahmi, H. M. Tarjam, and N. Ismail, "Skin protectant textiles loaded with fish collagen, chitosan and oak galls extract composite," *International Journal of Biological Macromolecules*, vol. 117, pp. 25–29, 2018.

[37] S. Vakilian, M. Norouzi, M. Soufi-Zomorrod, I. Shabani, S. Hosseinzadeh, and M. Soleimani, "*L. inermis*-loaded nanofibrous scaffolds for wound dressing applications," *Tissue and Cell*, vol. 51, pp. 32–38, 2018.

[38] Z. Hadisi, J. Nourmohammadi, and S. M. Nassiri, "The antibacterial and anti-inflammatory investigation of *Lawsonia inermis*-gelatin-starch nano-fibrous dressing in burn wound," *International Journal of Biological Macromolecules*, vol. 107, no. Part B, pp. 2008–2019, 2018.

[39] T. Nagai and N. Suzuki, "Isolation of collagen from fish waste material – skin, bone and fins," *Food Chemistry*, vol. 68, no. 3, pp. 277–281, 2000.

[40] L. C. Abraham, E. Zuena, B. Perez-Ramirez, and D. L. Kaplan, "Guide to collagen characterization for biomaterial studies," *Journal of Biomedical Materials Research Part B: Applied Biomaterials*, vol. 87B, no. 1, pp. 264–285, 2008.

[41] A. A. Tayel, A. F. Elzahy, S. H. Moussa, M. S. Al-Saggaf, and A. M. Diab, "Biopreservation of shrimps using composed edible coatings from chitosan nanoparticles and cloves extract," *Journal of Food Quality*, vol. 2020, 10 pages, 2020.

[42] A. Baxter, M. Dillon, K. A. Taylor, and G. A. Roberts, "Improved method for ir determination of the degree of N-acetylation of chitosan," *International Journal of Biological Macromolecules*, vol. 14, no. 3, pp. 166–169, 1992.

[43] A. C. Wu, "Determination of molecular-weight distribution of chitosan by high-performance liquid chromatography," *Methods in Enzymology*, vol. 161, pp. 447–452, 1988.

[44] S. Salamat, M. Hadavifar, and H. Rezaei, "Preparation of nanochitosan-STP from shrimp shell and its application in removing of malachite green from aqueous solutions," *Journal of Environmental Chemical Engineering*, vol. 7, no. 5, p. 103328, 2019.

[45] CLSI (Clinical and Laboratory Standard Institute), *Performance Standards for Antimicrobial Susceptibility Testing; 20th Informational Supplement. CLSI Document M100-S20. CLSI*, Clinical and Laboratory Standard Institute, Wayne, PA, 2010.

[46] T. Riaz, R. Zeeshan, F. Zarif et al., "FTIR analysis of natural and synthetic collagen," *Applied Spectroscopy Reviews*, vol. 53, no. 9, pp. 703–746, 2018.

[47] R. Duan, J. Zhang, X. Du, X. Yao, and K. Konno, "Properties of collagen from skin, scale and bone of carp (*Cyprinus carpio*)," *Food Chemistry*, vol. 112, no. 3, pp. 702–706, 2009.

[48] Z. I. Elbialy, A. Atiba, A. Abdelnaby et al., "Collagen extract obtained from Nile tilapia (*Oreochromis niloticus* L.) skin accelerates wound healing in rat model via up regulating VEGF, bFGF, and α-SMA genes expression," *BMC Veterinary Research*, vol. 16, p. 352, 2020.

[49] C. Y. Huang, J. M. Kuo, S. J. Wu, and H. T. Tsai, "Isolation and characterization of fish scale collagen from tilapia (*Oreochromis* sp.) by a novel extrusion–hydro-extraction process," *Food Chemistry*, vol. 190, pp. 997–1006, 2016.

[50] H. Avci, R. Monticello, and R. Kotek, "Preparation of antibacterial PVA and PEO nanofibers containing *Lawsonia inermis* (henna) leaf extracts," *Journal of Biomaterials Science, Polymer Edition*, vol. 24, pp. 1815–1830, 2013.

[51] N. H. Wagini, A. S. Soliman, M. S. Abbas, Y. A. Hanafy, and E. S. M. Badawy, "Phytochemical analysis of Nigerian and Egyptian henna (*Lawsonia inermis* L.) leaves using TLC, FTIR and GCMS," *Plant*, vol. 2, no. 3, pp. 27–32, 2014.

[52] I. Yousefi, M. Pakravan, H. Rahimi, A. Bahador, Z. Farshadzadeh, and I. Haririan, "An investigation of electrospun henna leaves extract-loaded chitosan based nanofibrous mats for skin tissue engineering," *Materials Science & Engineering. C, Materials for Biological Applications*, vol. 75, pp. 433–444, 2017.

[53] R. Davarnejad, Z. K. Dastnayi, and J. F. Kennedy, "Cr(VI) adsorption on the blends of henna with chitosan microparticles: experimental and statistical analysis," *International Journal of Biological Macromolecules*, vol. 116, pp. 281–288, 2018.

[54] P. D. Babu and R. S. Subhasree, "Antimicrobial activities of *Lawsonia inermis*-a review," *Academic Journal of Plant Sciences*, vol. 2, pp. 231-232, 2009.

[55] W. Raja, M. Ovais, and A. Dubey, "Phytochemical screening and antibacterial activity of *Lawsonia inermis* leaf extract," *International Journal of Microbiology Research*, vol. 4, pp. 33–36, 2016.

[56] U. Shivsharan and Y. Kothari, "Antimicrobial activity and isolation of lawsone from *Lawsonia inermis* using column chromatography," *Research Journal of Pharmacognosy and Phytochemistry*, vol. 12, pp. 219–223, 2020.

[57] T. Singam, N. B. Marsi, A. H. B. Abdul Rashid et al., "A review on characteristics and potential applications of henna leaves (*Lawsonia inermis*)," *Journal of Computational and Theoretical Nanoscience*, vol. 17, pp. 603–612, 2020.

[58] F. M. Almutairi, H. A. El Rabey, A. A. Tayel et al., "Augmented anticancer activity of curcumin loaded fungal chitosan nanoparticles," *International Journal of Biological Macromolecules*, vol. 155, pp. 861–867, 2020.

[59] A. I. Alalawy, H. A. El Rabey, F. M. Almutairi et al., "Effectual anticancer potentiality of loaded bee venom onto fungal chitosan nanoparticles," *International Journal of Polymer Science*, vol. 2020, 9 pages, 2020.

[60] M. M. Mihai, M. B. Dima, B. Dima, and A. M. Holban, "Nanomaterials for wound healing and infection control," *Materials*, vol. 12, no. 13, p. 2176, 2019.

[61] M. Yanat and K. Schroën, "Preparation methods and applications of chitosan nanoparticles; with an outlook toward reinforcement of biodegradable packaging," *Reactive and Functional Polymers*, vol. 161, p. 104849, 2021.

[62] J. Y. Yang and H. S. Lee, "Antimicrobial activities of active component isolated from *Lawsonia inermis* leaves and structure-activity relationships of its analogues against foodborne bacteria," *Journal of Food Science and Technology*, vol. 52, no. 4, pp. 2446–2451, 2015.

[63] S. Hamdan, I. Pastar, S. Drakulich et al., "Nanotechnology-driven therapeutic interventions in wound healing: potential uses and applications," *ACS Central Science*, vol. 3, no. 3, pp. 163–175, 2017.

[64] M. E. Okur, I. D. Karantas, Z. Şenyiğit, N. Ü. Okur, and P. I. Siafaka, "Recent trends on wound management: new therapeutic choices based on polymeric carriers," *Asian Journal of Pharmaceutical Sciences*, vol. 15, no. 6, pp. 661–684, 2020.

[65] A. C. Gonzalez, T. F. Costa, Z. D. Andrade, and A. R. Medrado, "Wound healing-a literature review," *Anais Brasileiros de Dermatologia*, vol. 91, no. 5, pp. 614–620, 2016.

[66] T. D. Nguyen, T. T. Nguyen, K. L. Ly et al., "*In vivo* study of the antibacterial chitosan/polyvinyl alcohol loaded with silver nanoparticle hydrogel for wound healing applications," *International Journal of Polymer Science*, vol. 2019, 10 pages, 2019.

[67] C. A. Fleck and R. Simman, "Modern collagen wound dressings: function and purpose," *Journal of the American College of Certified Wound Specialists*, vol. 2, no. 3, pp. 50–54, 2010.

[68] T. Zhou, N. Wang, Y. Xue et al., "Electrospun tilapia collagen nanofibers accelerating wound healing via inducing keratinocytes proliferation and differentiation," *Colloids and Surfaces B: Biointerfaces*, vol. 143, pp. 415–422, 2016.

[69] J. Chen, K. Gao, S. Liu et al., "Fish collagen surgical compress repairing characteristics on wound healing process in vivo," *Marine Drugs*, vol. 17, no. 1, p. 33, 2019.

[70] B. R. Mikhaeil, F. A. Badria, G. T. Maatooq, and M. M. A. Amer, "Antioxidant and immunomodulatory constituents of henna leaves," *Zeitschrift für Naturforschung C. A Journal of Biosciences*, vol. 59, no. 7-8, pp. 468–476, 2004.

[71] K. Rohini and S. P. Srikumar, "Therapeutic role of coumarins and coumarin-related compounds," *Journal of Thermodynamics and Catalysis*, vol. 5, no. 1, p. 130, 2014.

[72] I. Nounaha, A. Hajib, H. Harhar et al., "Chemical composition and antioxidant activity of *Lawsonia inermis* seed extracts from Morocco," *Natural Product Communications*, vol. 12, no. 4, pp. 1934578X1701200–1934578X1701488, 2017.